

Review of ATLAS Higgs \rightarrow WW Results with 25 fb⁻¹ of Data

Nikolina Ilic¹

University of Toronto Department of Physics

60 St. George St, Toronto, Ontario, Canada

E-mail: Nikolina.Ilic@cern.ch

The search for the Higgs boson in the WW channel is presented using data samples collected in 2011 and 2012 with the ATLAS detector [1] at the LHC. The data collected corresponds to 4.6 fb⁻¹ and 20.7 fb⁻¹ collected at a center-of-mass energy of 7 TeV and 8 TeV, respectively. The search focuses on a Higgs boson predicted by the Standard Model and produced by gluon-gluon fusion and vector boson fusion. At a Higgs mass of $m_H = 125$ GeV, an excess over the expected number of background events is expected to be 3.7 standard deviations, while the observed is 3.8. The ratio of the observed number of events to the expected is $\mu = 1.01 \pm 0.31$ for the combined searches in the $e\mu, ee, \mu\mu$ channel for 0, 1 and ≥ 2 jet multiplicities. A coupling measurement performed is shown to be consistent with the value predicted by the Standard Model. Finally a spin analysis is described which supports evidence for a Higgs particle of spin 0⁺.

The XXI International Workshop High Energy Physics and Quantum Field Theory

June 23 – June 30, 2013

Saint Petersburg Area, Russia

¹

1. Introduction

These proceedings focus on the search for Higgs boson in the WW channel when the Higgs is created through gluon-gluon fusion (ggF) and vector boson fusion (VBF) as shown in Figure 1. When the Higgs is created through the ggF process, the final decay state consists of two leptons, two neutrinos and possibly a jet from initial or final state radiation. When the Higgs is created via the VBF process, the final state consists of two leptons and neutrinos from the Higgs decay, as well as two forward jets from the initial quarks. The search is separated by lepton flavors and jet multiplicities, with final states being defined by different flavor ($e\mu/\mu e$) and same flavor ($ee/\mu\mu$) channels in 0, 1 and ≥ 2 jet multiplicities.

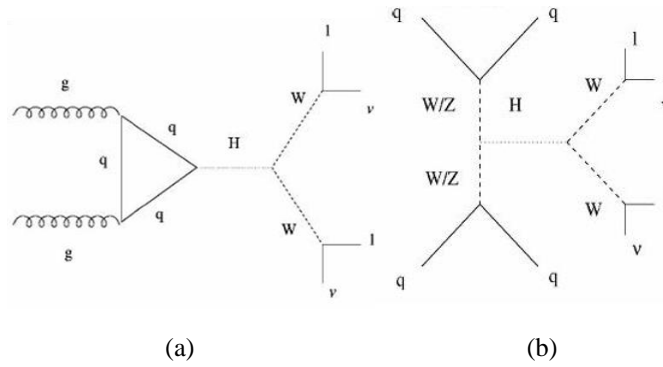


Figure 1 : The Feynman diagrams representing ggF on the left, and VBF on the right

2. Background Reduction and Signal Extraction

The primary background processes to ggF and VBF Higgs production are W +jets, $W\gamma$, $W\gamma^*$, WZ , ZZ , $Z/\gamma^* + \text{jets}$, top, and WW . In order to extract the signal events from the backgrounds, the backgrounds are reduced by topological selections. These selections, presented in Table 1, are described in subsequent subsections.

2.1 W +jets Estimation and Reduction

The W +jets processes, shown in Figure 2 (a), contain kinematic distributions similar to the signal signature when one of the jets is misidentified as a lepton. The small W +jets background remaining after the two lepton requirement is made is difficult to model in Monte Carlo. Thus it is estimated using a data driven method from a control region. The control region is defined as events which contain one lepton that passes the requirements for a good quality lepton, and another which fails some of these requirements, denoted as the denominator lepton. The amount of W +jets is then estimated in the signal region using equation (1).

$$N_{w+j}^{SR} = f \times N_{w+j}^{CR}, \text{ where } f = \frac{N_{\text{Good Lepton}}}{N_{\text{Denominator}}} \quad (1)$$

In equation (1), the fake factor, f , is estimated as a function of the denominator lepton transverse momentum, p_T , and pseudorapidity, η , from a di-jet sample. The fake factor has a 45% (40%) uncertainty from misidentified electrons (muons) due to differences between the di-jet and W +jets samples, pileup and real lepton contamination from W/Z boson events. The W +jets estimation also includes the QCD background estimation, when both leptons are misidentified as

jets. A validation region with same sign leptons containing mostly W +jets is used to validate the W +jets estimation. The W +jets backgrounds are reduced by selecting events with higher values of the missing transverse energy, E_T^{miss} , or its projection on the direction of the nearest reconstructed object, $E_{T,\text{rel}}^{\text{miss}}$.

Table 1: The topological selections applied for background rejection and signal extraction for 8 TeV data [2].

Category	$N_{\text{jet}} = 0$	$N_{\text{jet}} = 1$	$N_{\text{jet}} \geq 2$
Pre-selection	Two isolated leptons ($\ell = e, \mu$) with opposite charge Leptons with $p_T^{\text{lead}} > 25$ and $p_T^{\text{sublead}} > 15$ $e\mu + \mu e: m_{\ell\ell} > 10$ $ee + \mu\mu: m_{\ell\ell} > 12, m_{\ell\ell} - m_Z > 15$		
Missing transverse momentum and hadronic recoil	$e\mu + \mu e: E_{T,\text{rel}}^{\text{miss}} > 25$ $ee + \mu\mu: E_{T,\text{rel}}^{\text{miss}} > 45$ $ee + \mu\mu: p_{T,\text{rel}}^{\text{miss}} > 45$ $ee + \mu\mu: f_{\text{recoil}} < 0.05$	$e\mu + \mu e: E_{T,\text{rel}}^{\text{miss}} > 25$ $ee + \mu\mu: E_{T,\text{rel}}^{\text{miss}} > 45$ $ee + \mu\mu: p_{T,\text{rel}}^{\text{miss}} > 45$ $ee + \mu\mu: f_{\text{recoil}} < 0.2$	$e\mu + \mu e: E_T^{\text{miss}} > 20$ $ee + \mu\mu: E_T^{\text{miss}} > 45$ $ee + \mu\mu: E_{T,\text{STVF}}^{\text{miss}} > 35$ -
General selection	- $ \Delta\phi_{\ell\ell, \text{MET}} > \pi/2$ $p_T^{\ell\ell} > 30$	$N_{b\text{-jet}} = 0$ - $e\mu + \mu e: Z/\gamma^* \rightarrow \tau\tau$ veto	$N_{b\text{-jet}} = 0$ $p_T^{\text{tot}} < 45$ $e\mu + \mu e: Z/\gamma^* \rightarrow \tau\tau$ veto
VBF topology	- - - -	- - - -	$m_{jj} > 500$ $ \Delta y_{jj} > 2.8$ No jets ($p_T > 20$) in rapidity gap Require both ℓ in rapidity gap
$H \rightarrow WW^{(*)} \rightarrow \ell\nu\ell\nu$ topology	$m_{\ell\ell} < 50$ $ \Delta\phi_{\ell\ell} < 1.8$ $e\mu + \mu e$: split $m_{\ell\ell}$ Fit m_T	$m_{\ell\ell} < 50$ $ \Delta\phi_{\ell\ell} < 1.8$ $e\mu + \mu e$: split $m_{\ell\ell}$ Fit m_T	$m_{\ell\ell} < 60$ $ \Delta\phi_{\ell\ell} < 1.8$ - Fit m_T

2.2 Non WW Diboson (W_Y, W_Y^*, WZ, ZZ) Estimation and Reduction

The non WW diboson backgrounds, shown in Figure 2 (b), usually produce three leptons in the final state and are largely reduced once two leptons of opposite charge are selected. This background is small and estimated from Monte Carlo. The accuracy of the modeling of non WW dibosons is cross checked using a same sign validation region. The uncertainty on the non WW diboson background estimation in the signal region is 16% (22%) for the 0 (1) jet channel.

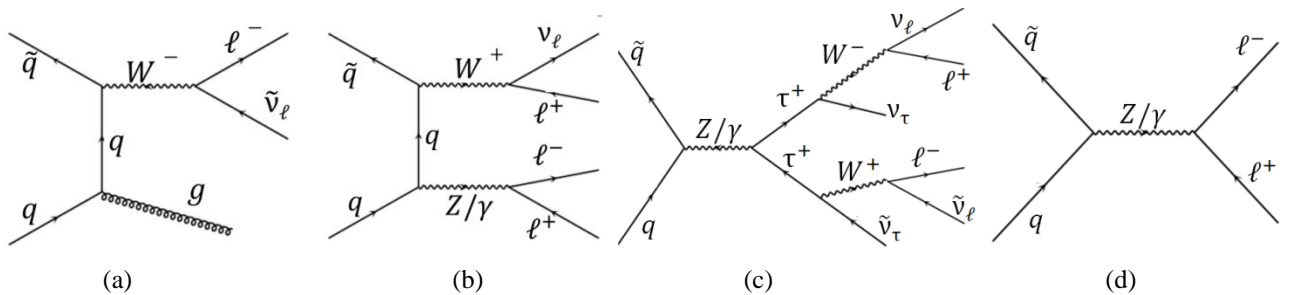


Figure 2 : The Feynman diagrams for the W +jets background in (a), non WW Diboson background in (b), $Z/\gamma^* \rightarrow \tau^+\tau^-$ background in (c), and $Z/\gamma^* \rightarrow \ell^+\ell^-$ background in (d).

2.3 $Z/\gamma^* + \text{jets}$ Estimation and Reduction

The $Z/\gamma^* + \text{jets}$ background is significant in the different flavor channel when the Z/γ^* decays to $\tau^+\tau^-$ (Figure 2 (c)), and significant for the same flavor channel when the Z/γ^* decays to $\ell^+\ell^-$ (Figure 2 (d)). The $Z/\gamma^* \rightarrow \tau^+\tau^-$ background is estimated from a control region defined by selecting events whose invariant di-lepton mass, $m_{\ell\ell}$, is low, and whose opening angle between the leptons, $\Delta\phi_{\ell\ell}$, is high. The $Z/\gamma^* \rightarrow \ell\ell$ background is small for different flavor and is thus taken from Monte Carlo. The $Z/\gamma^* \rightarrow \ell\ell$ background is large for same flavor and is estimated and reduced by exploiting soft hadronic recoil opposing the di-leptons in the transverse plane, f_{recoil} . The $Z/\gamma^* + \text{jets}$ background is reduced by removing events around the Z mass peak ($Z \rightarrow \tau^+\tau^-$ veto), removing events with lower $E_T^{miss}/E_{T,rel}^{miss}$, and, in the 0 jet channel, removing events with higher transverse mass of the leptons, $p_T^{\ell\ell}$. The same flavor channel also makes requirements on missing transverse energy calculated from tracks in the inner detector, p_T^{miss} , which is less sensitive to pileup effects.

2.4 Top Background Estimation and Reduction

The top background consists of single top and $t\bar{t}$ events as shown in Figure 3 (a) and (b). These events can enter the signal region when the bottom quarks decay leptonically, are missed or are misidentified as leptons. The top background is modeled by Monte Carlo and corrected to data from a control region which contains bottom tagged jets, N_{b-jet} . This background is reduced by requiring N_{b-jet} to be 0, and for the ≥ 2 j channel, selecting on low values of the total transverse momentum, p_T^{tot} .

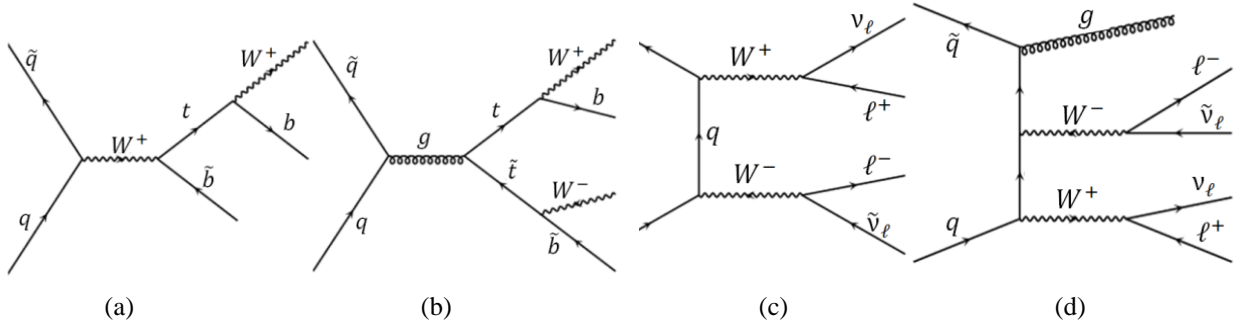


Figure 3: The Feynman diagrams for single top background in (a), $t\bar{t}$ background in (b), WW background in the 0 jet channel in (c) and WW background in the 1 jet channel in (d).

2.5 WW Background Estimation and Rejection

The WW background, shown in Figure 3 (c) and (d), has the same final states and similar kinematic distributions as the signal. It is modeled by Monte Carlo and corrected to data from a control region for 0/1 jet channels, and is taken directly from Monte Carlo for the ≥ 2 jet channel due to a lack of statistics in the control region. The $m_{\ell\ell}$ distribution, expected to peak at 80 GeV for WW events, is also used to separate the WW control region from the signal region. Another good discriminant used to define the control region, and reduce the WW background in the signal region is $\Delta\phi_{\ell\ell}$. Unlike for the WW background, $\Delta\phi_{\ell\ell}$ is small for the Higgs since it is a spin 0 particle and the spin of the two bosons is correlated.

2.6 Signal Extraction

After topological selections are made to reduce the backgrounds, further criteria are implemented to extract the signal by selecting on variables specific to the signal topology. In ggF production the signal topology is extracted by selecting on low values of $m_{\ell\ell}$ and $\Delta\phi_{\ell\ell}$. The ggF signal region is split into two $m_{\ell\ell}$ regions ($0 \text{ GeV} < m_{\ell\ell} < 30 \text{ GeV}$ and $30 \text{ GeV} < m_{\ell\ell} < 50 \text{ GeV}$) in order to gain better sensitivity by exploiting the different signal over background ratios in these regions.

In VBF production the energetic final state jets are in the forward regions of the detector. Thus in order to extract the VBF signal, requirements are made on the invariant mass of the two jets, m_{jj} , and the rapidity gap between them, Δy_{jj} (Table 1). In addition to this, no jets are required to be inside the rapidity gap.

The signal strength is measured using the transverse mass, m_T , distribution as defined in equation (2) and (3).

$$m_T = \left(\left(E_T^{\ell\ell} + E_T^{\text{miss}} \right)^2 - \left| \mathbf{p}_T^{\ell\ell} - E_T^{\text{miss}} \right|^2 \right)^{1/2} \quad (2)$$

$$E_T^{\ell\ell} = \left(\left| \mathbf{p}_T^{\ell\ell} \right|^2 + m_{\ell\ell}^2 \right)^{1/2} \quad (3)$$

The m_T distribution is shown in Figure 4. Table 2, shows the number of background, signal and data events after the selections to reduce the backgrounds are applied.

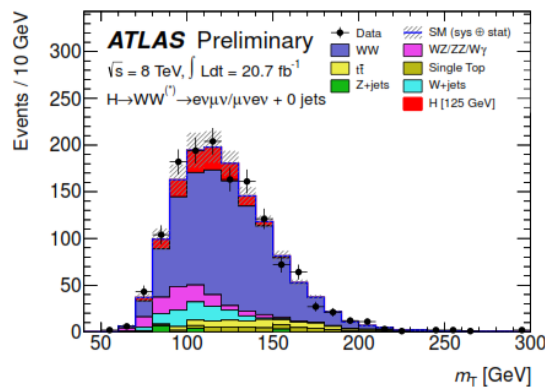


Figure 4: The transverse mass distribution after selections described in Table 1 [3].

Table 2: Events in the m_T range of highest expected signal over background, $0.75 m_H < m_T < m_H$ for $N_{jet} \leq 1$, and $m_T < 1.2 m_H$ for $N_{jet} \geq 2$ [2].

N_{jet}	N_{obs}	N_{bkg}	N_{sig}
$= 0$	831	739 ± 39	97 ± 20
$= 1$	309	261 ± 28	40 ± 13
≥ 2	55	36 ± 4	10.6 ± 1.4

3. Results

3.1 7 TeV and 8 TeV Combined results

The statistical analysis is performed using the likelihood function, \mathcal{L} , which is defined using the m_T distribution. The likelihood is a product, of Poisson functions over the signal and control regions and Gaussian constraints. The parameter of interest, μ , in the Poisson distribution is a scale factor representing the expected signal yield, with $\mu = 0$ corresponding to background only hypothesis, and $\mu = 1$ corresponding to the SM predicted signal hypothesis. This parameter moves freely to best fit the data. The expected signal and background yields are also allowed to move freely within the allowed range of their systematic uncertainties. These systematic uncertainties are parameterized by nuisance parameters, θ , that are constrained by Gaussian distributions. To compute the 95% confidence level exclusions and the p_0 value, the modified

frequentist method (CLs) is used [3]. The resulting limit and p_0 plots are shown in Figure 5. Figure 5 (a) shows that the highest expected significance of 4.1 s.d. ($p_0 = 2 \times 10^{-5}$) occurs when the signal has a Higgs mass of 140 GeV. The expected and observed significances for a Higgs mass of 125 GeV are 3.7 s.d. ($p_0 = 10^{-4}$) and 3.8 s.d. ($p_0 = 8 \times 10^{-5}$) respectively. Figure 5 (b) shows that a standard model Higgs boson is expected to be excluded at a 95% confidence level for $m_H < 119$ GeV, while the observed exclusion is $m_H < 133$ GeV.

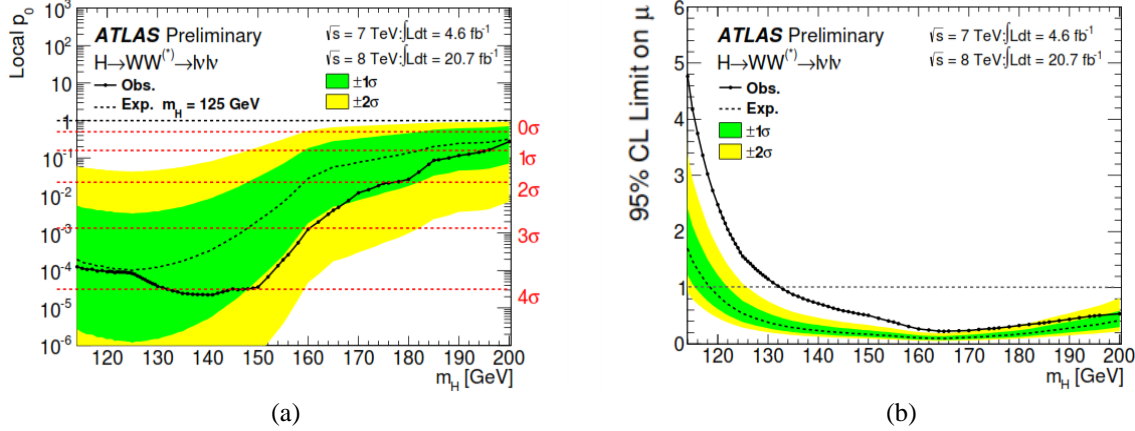


Figure 5: The p_0 value in (a) and 95% confidence level plot in (b) in the $0, 1 \geq 2$ jet channels in $e\mu, ee, \mu\mu$ for the 7 TeV and 8 TeV analyses [2].

The signal strength, obtained by maximizing \mathcal{L} , is the ratio of the observed number of events to the expected and is given by

$$\begin{aligned} \mu_{obs} &= 1.01 \pm 0.21 \text{ (stat.)} \pm 0.19 \text{ (theo. syst.)} \pm 0.21 \text{ (expt. syst.)} \pm 0.04 \text{ (lumi.)} \\ &= 1.01 \pm 0.31 \end{aligned}$$

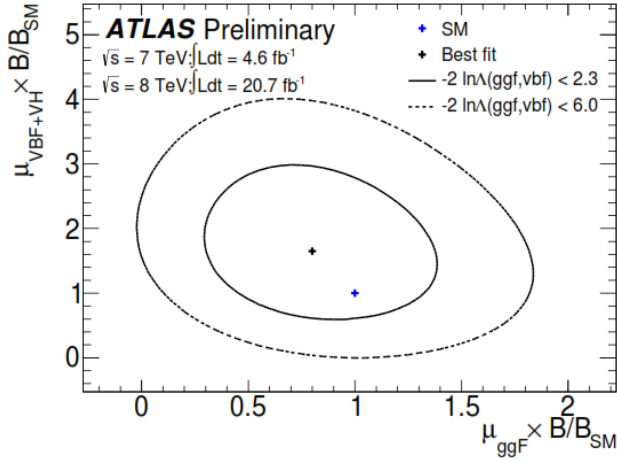
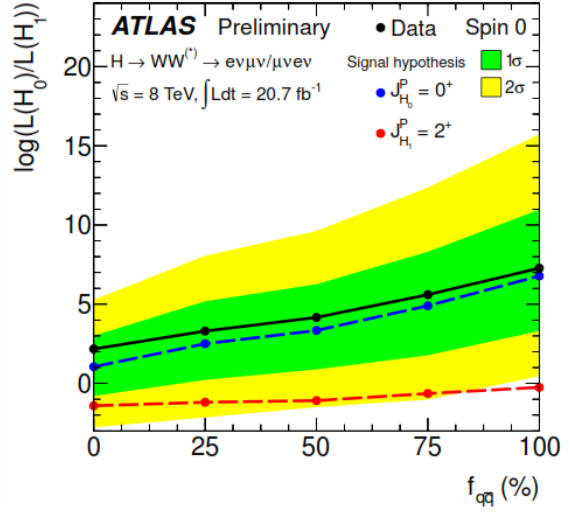
for a Higgs mass of 125 GeV for the 7 and 8 TeV combined data. The dominant systematic uncertainties are the theoretical uncertainties such as the WW background normalization, signal cross sections and branching ratios, as well as the experimental uncertainties associated with the b-tagging efficiencies, and jet energy scale and resolution.

3.2 Coupling Results

In order to obtain a coupling measurement, the VBF signal strength, μ_{VBF} , is measured in the ≥ 2 jet channel by considering ggF as a background process. Similarly the ggF signal, μ_{ggF} , is measured by considering VBF as a background processes. The values for the signal strengths are

$$\begin{aligned} \mu_{obs,VBF} &= 1.66 \pm 0.67 \text{ (stat.)} \pm 0.42 \text{ (syst.)} = 1.66 \pm 0.79 \\ \mu_{obs,ggF} &= 0.82 \pm 0.24 \text{ (stat.)} \pm 0.28 \text{ (syst.)} = 0.82 \pm 0.36 \end{aligned}$$

Figure 7 is a two dimensional likelihood scan of the signal strength for ggF and VBF production modes. The Higgs associated production modes, WH and ZH, are also grouped with VBF since these modes scale with the VH coupling. This plot shows that the coupling measurement is consistent with the standard model expectation of one.

Figure 7: Likelihood curves for μ_{VBF+VH} and $\mu_{ggF+ttH}$ [2].Figure 8: The test statistic as a function of $f_{q\bar{q}}$ to test the spin 0^+ versus spin 2^+ hypotheses [4].

4. Spin

The measurement of the spin within the Higgs to WW search attempts to differentiate between a Higgs with spin 0^+ and a graviton-like spin 2^+ particle. This analysis focuses on the different flavor, 0 jet channel and 2012 data. It uses a Boosted Decision Tree (BDT) method [4] to train four variables (m_T , $\Delta\varphi_{\ell\ell}$, $m_{\ell\ell}$, $p_T^{\ell\ell}$) to use in signal and background discrimination. For the spin 2^+ scenario the fraction of gg and $q\bar{q}$ production is unknown. Thus a scan is performed over five different fractions, $f_{q\bar{q}}$, in which the percentage of $q\bar{q}$ production relative to gg is 0%, 25%, 50%, 75%, and 100%. The compatibility between the data and two hypotheses is tested using the test statistic shown in equation (4).

$$q = \log \frac{\mathcal{L}(H_{0^+})}{\mathcal{L}(H_{2^+})} = \log \frac{\mathcal{L}(\epsilon=1, \hat{\mu}_{\epsilon=1}, \hat{\theta}_{\epsilon=1})}{\mathcal{L}(\epsilon=0, \hat{\mu}_{\epsilon=0}, \hat{\theta}_{\epsilon=0})} \quad (4)$$

In equation (4) the parameter of interest, ϵ represents the expected number of spin 0 relative to the total number of signal events, with $\epsilon=0$ representing the spin 2^+ and $\epsilon=1$ representing the spin 0^+ hypotheses respectively. Figure 8 shows the scan of the test statistics versus $f_{q\bar{q}}$. The data, represented by the black line in Figure 8, are compatible with the spin 0^+ hypothesis, represented by the blue line. The spin 2^+ hypothesis is excluded at a 99% confidence level for $q\bar{q}$ production, and 95% confidence level for gg production.

5. Conclusion

A search for the Higgs boson in the $e\mu, ee, \mu\mu$ channel for 0, 1 and ≥ 2 jet multiplicities with 7 TeV and 8 TeV data is presented. At a hypothesized Higgs mass of $m_H = 125$ GeV, an excess over the expected number of background events is expected (observed) to be 3.7 (3.8) s.d, while the measured signal strength is $\mu = 1.01 \pm 0.31$. The coupling measurement is consistent with the Standard Model value. The spin analysis performed supports evidence for a Higgs particle of spin 0^+ .

References

- [1] ATLAS Collaboration, *The ATLAS Experiment at the CERN Large Hadron Collider*, 2008 *JINST* **3** S08003
- [2] The ATLAS Collaboration, *Measurements of the properties of the Higgs-like boson in the $WW \rightarrow \ell\nu\ell\nu$ decay channel with the ATLAS detector using 25fb^{-1} of proton-proton collision data*. ATLAS-CONF-2013-030
- [3] The ATLAS Collaboration, *Study of the spin properties of the Higgs-like boson in the $H \rightarrow WW \rightarrow e\nu\mu\nu$ channel with 21fb^{-1} of $\sqrt{s} = 8 \text{ TeV}$ data collected with the ATLAS detector*. ATLAS-CONF-2013-31
- [4] G. Cowan, K. Cranmer, E. Gross, and O. Vitells, *Asymptotic formulae for likelihood-based tests of new physics*, *Eur. Phys. J.* **C71** (2011) 1554

POS(QFTHEP 2013)025